Temporal Dynamics of Normalization Reweighting

Daniel H. Baker, Daniela Marinova, Richard Aveyard, Lydia J. Hargreaves, Alice Renton, Ruby Castellani, Phoebe Hall, Miriam Harmens, Georgia Holroyd, Beth Nicholson, Emily L. Williams, Hannah M. Hobson & Alex R. Wade

Department of Psychology, University of York, UK

1 Abstract

For decades, neural suppression in early visual cortex has been thought to be fixed. But recent work has challenged this assumption by showing that suppression can be *reweighted* based on recent history; when pairs of stimuli are repeatedly presented together, suppression between them strengthens. Here we investigate the temporal dynamics of this process using a steady-state visual evoked potential (SSVEP) paradigm that provides a time-resolved, direct index of suppression between pairs of stimuli flickering at different frequencies (5 and 7Hz). Our initial analysis of an existing EEG dataset (N=100) indicated that suppression increases substantially during the first 2-5 seconds of stimulus presentation (with some variation across stimulation frequency). We then collected new EEG data (N=100) replicating this finding for both monocular and dichoptic mask arrangements in a preregistered study designed to measure reweighting. A third experiment (N=20) used source localized MEG, and found that these effects are apparent in primary visual cortex (V1), consistent with results from neurophysiological work. Because long-standing theories propose inhibition/excitation differences in autism, we also compared reweighting between individuals with high vs low autistic traits, and with and without an autism diagnosis, across our 3 data sets (total N=220). We find no compelling differences in reweighting that are associated with autism. Our results support the normalization reweighting model, and indicate that for prolonged stimulation, increases in suppression occur on the order of 2-5 seconds after stimulus onset.

2 Significance statement

We investigated the timecourse of a novel form of neural plasticity, normalization reweighting, using steady-state EEG in humans. We find increases in suppression during the first 2-5 seconds of stimulation, with similar dynamics for monocular and dichoptic presentation. The effects are present in primary visual cortex, and were not mediated by autistic traits. These findings demonstrate that reweighting builds up rapidly after stimulus onset, consistent with a process that adjusts the sensory response to the local environment. Normalization reweighting also has potential as a biomarker of neural function both in humans and in animal models of disease.

3 Introduction

Suppressive interactions between neurons are ubiquitous in the nervous system, with normalization considered a canonical neuronal computation (Carandini and Heeger, 2011). Yet for decades the strength of suppression was treated as fixed, due to the observation that adapting to one stimulus does not decrease its suppressive potency (Foley and Chen, 1997; Freeman et al., 2002). This orthodoxy has been challenged by a series of innovative studies showing that normalization can be 'reweighted' by recent history (Aschner et al., 2018; Westrick et al., 2016; Yiltiz et al., 2020). When pairs of stimuli are repeatedly presented together, their neural representations come to suppress each other more strongly. Far from being fixed, normalization is therefore a dynamic process that is continuously updated by the sensory environment. Our objectives were

to measure the timecourse of these changes non-invasively in the human brain, compare them across distinct suppressive pathways, and determine whether they differ as a function of autistic traits.

Plastic changes within the visual system occur over multiple timescales (see Webster, 2015 for a recent review). Cortical forms of adaptation to cues such as stimulus contrast (Blakemore and Campbell, 1969), orientation (Gibson and Radner, 1937) and motion (Mather et al., 2008) can be observed within a few seconds, but also build up over durations on the order of minutes (Greenlee et al., 1991). Other types of adaptation have been identified where changes occur over longer time periods, such as several hours (Kwon et al., 2009) or days (Haak et al., 2014). Previous normalization reweighting studies involved adapting sequences of around 40 – 60s (Aschner et al., 2018; Yiltiz et al., 2020), but in principle reweighting might occur faster than this, consistent with other types of contrast adaptation.

Multiple suppressive pathways have been identified in the visual system, including between stimuli differing in orientation (Foley, 1994; Heeger, 1992), eye-of-origin (Legge, 1979; Sengpiel and Blakemore, 1994) and spatial position (Cannon and Fullenkamp, 1991; Petrov, 2005). At present there is evidence of normalization reweighting between stimuli with orthogonal orientations (Aschner et al., 2018), and adjacent spatial positions (Yiltiz et al., 2020). We anticipated that interocular suppression should also be subject to reweighting, but that there might be differences in the dynamics across suppressive pathways (Li et al., 2005; e.g. Meese and Baker, 2009; Sengpiel and Vorobyov, 2005). Comparing monocular and dichoptic suppression permits any contribution of early pre-cortical factors to be isolated. This is because interocular suppression impacts in primary visual cortex, and bypasses any retinal and subcortical stages of processing that contribute to monocular suppression (Li et al., 2005).

Atypical sensory experience, including hypersensitivity to loud sounds, bright lights and strong odours or flavours, is widely reported by individuals on the autism spectrum (MacLennan et al., 2022; Simmons et al., 2009), but the causal mechanisms remain unclear. Fundamental measures of sensitivity including visual acuity (Tavassoli et al., 2011), contrast sensitivity (Koh et al., 2010), and audiometric performance (Rosenhall et al., 1999) are not consistently different from neurotypical controls. Theoretical accounts of sensory differences in autism have proposed that the balance of inhibition and excitation may be disrupted (Rosenberg et al., 2015; Rubenstein and Merzenich, 2003), yet the evidence is currently inconclusive (Sandhu et al., 2020; e.g. Schallmo et al., 2020; Van de Cruys et al., 2018). Our recent work identified an autism-related difference using steady-state EEG (Vilidaite et al., 2018), in which nonlinear (second harmonic) responses were weaker, implicating atypical suppression in autism.

Here we perform a time-course analysis of a previously published data set, and report two novel pre-registered experiments using EEG and MEG. Our data show that suppression increases substantially during the first 2-5 seconds following stimulus onset, for both monocular and dichoptic masks. Source localisation of MEG data indicate that the reweighting is present as early as primary visual cortex (V1). We also hypothesised that normalization reweighting might differ as a function of autistic traits, but did not find convincing support for this hypothesis.

4 Materials and Methods

4.1 Participants

Experiment 1 was completed by 100 adult participants (32 male, 68 female; mean age 21.9) in early 2015, and first reported by Vilidaite et al. (2018). Here we reanalysed the dataset, and report the results of masking conditions not previously published. Experiment 2 was completed by 100 adult participants (23 male, 74 female, 3 other/not stated; mean age 22.1) in early 2022. Experiment 3 was completed by 10 adults (2 male, 8 female) with a clinical diagnosis of autism, and 10 control participants who were closely matched for age (means of 21.8 and 22, $t = 0.18$, $df = 18$, $p = 0.86$) and exactly matched for gender. Procedures in Experiments 1 and 2 were approved by the ethics committee of the Department of Psychology at the University of York. Procedures for Experiment 3 were approved by the ethics committee of the York Neuroimaging Centre. All participants provided written informed consent.

4.2 Apparatus and stimuli

In Experiments 1 and 2, stimuli were presented using a ViewPixx 3D LCD display device (VPixx Technologies, Canada) with a resolution of 1920 × 1080 pixels and a refresh rate of 120Hz. The display was gamma corrected using a Minolta LS110 photometer. In Experiment 2, participants wore active stereo shutter glasses (NVidia 3D Vision 2) that were synchronised with the display using an infra-red signal. EEG data were collected using a 64-channel Waveguard cap, and were amplified and digitised at 1000Hz using an ANT Neuroscan system. Electrode impedance was maintained below 5kΩ, and referenced to a whole-head average.

In Experiment 3, stimuli were presented using a ProPixx DLP projector (VPixx Technologies) running at 120Hz. Stereo presentation was enabled using a circular polariser that was synchronised with the projector refresh, and participants wore passive polarised glasses during the experiment. DLP projectors are perfectly linear, so gamma correction was not required. Data were acquired using a refurbished 248-channel 4D Neuroimaging Magnes 3600 MEG scanner, recording at 1001Hz. Participant head shape was digitised using a Polhemus Fastrak device, and head position was recorded at the start and end of each block by passing current through 5 position coils placed at fiducial points on the head. We also obtained structural MRI scans using a 3 Tesla Siemens Magnetom Prisma scanner to aid in source localisation. Two participants were not available for MRI scans, so we used the MNI ICBM152 template brain (Fonov et al., 2011) for these individuals.

Stimuli were patches of sine wave grating with a diameter of 2 degrees, flickering sinusoidally (on/off flicker) at either 5Hz or 7Hz. In Experiment 1 the gratings had a spatial frequency of 0.5c/deg, and in Experiments 2 & 3 this was increased to 2c/deg. A symmetrical array of 36 individual patches tiled the display. In Experiment 1 the patch orientation was randomly selected on each trial, and all patches had the same orientation. In Experiments 2 & 3 each patch had a random orientation, which was intended to prevent any sequential effects between trials with similar orientations. The central patch was omitted and replaced by a fixation marker constructed from randomly overlaid squares. During each experiment, the fixation marker could be resampled on each trial with a probability of 0.5. Participants were instructed to monitor the fixation marker and count the number of times it changed throughout the experiment. This was intended to maintain attention towards the display and keep participants occupied.

Participants also completed either the short AQ (Hoekstra et al., 2011) in Experiment 1, or the full AQ (Baron-Cohen et al., 2001) in Experiments 2 and 3. For comparison across experiments, we rescaled the short AQ to the same range as the full AQ (0-50). In Experiments 2 and 3, the sensory perception quotient (SPQ) questionnaire (Tavassoli et al., 2014) was also completed.

4.3 Experimental design and statistical analysis

In Experiment 1, target stimuli flickering at 7Hz were presented at a range of contrasts (1 - 64%). In half of the conditions a superimposed orthogonal mask of 32% contrast was presented simultaneously, flickering at 5Hz. Stimuli were displayed for trials of 11 seconds, with a 3 second inter-trial interval. The experiment consisted of 4 blocks of trials, each lasting around 10 minutes, and resulting in 8 repetitions of each condition. Participants viewed the display from 57cm, were comfortably seated in an upright position, and were able to rest between blocks. Low latency 8-bit digital triggers transmitted the trial onset and condition information directly to the EEG amplifier.

The procedure for Experiment 2 was very similar, except that participants also wore stereo shutter glasses during the experiment. There were four conditions: (i) monocular presentation of a 5Hz stimulus of 48% contrast, (ii) monocular presentation of a 7Hz stimulus of 48% contrast, (iii) monocular presentation of both stimuli superimposed at right angles, and (iv) dichoptic presentation of both stimuli at right angles (i.e. one stimulus to the left eye, one to the right eye). Eye of presentation was pseudo-randomised to ensure equal numbers of left-eye and right-eye presentations. The trial duration was 6 seconds, with a 3 second inter-trial interval. Participants completed 3 blocks, each lasting around 10 minutes, resulting in a total of 48 repetitions of each condition. Experiment 3 was identical, except that the projector screen was viewed from a distance of 85cm.

EEG data from Experiments 1 and 2 were first imported into Matlab using components of the EEGlab

toolbox (Delorme and Makeig, 2004), and converted into a compressed ASCII format. Primary data analysis was then conducted using a bespoke *R* script. In brief, we epoched each trial and extracted the average timecourse across four occipital electrodes (*Oz*, *POz*, *O1* and *O2*), and then calculated the Fourier transform of this average waveform. We excluded trials for which the Mahalanobis distance of the complex Fourier components exceeded 3 (for details see Baker, 2021). This resulted in 0.25% of trials being excluded for Experiment 1, and 4.51% of trials for Experiment 2. Next we averaged the waveforms across all remaining trials, and calculated the Fourier transform in a 1-second sliding window to generate timecourses for each participant. We divided the timecourse for the target-only condition by the timecourse for the target + mask condition to produce a suppression ratio. These were then converted to logarithmic (dB) units for averaging, calculation of standard errors, and statistical comparisons. For display purposes we smoothed the timecourses using a cubic spline function, however all statistical comparisons used the unsmoothed data.

For Experiment 3, we performed source localisation using a linearly constrained minimum variance (LCMV) beamformer algorithm, implemented in Brainstorm (Tadel et al., 2011). Structural MRI scans were processed using Freesurfer (Dale et al., 1999) to generate a 3D mesh of the head and brain, and we calculated source weights for each block with reference to a 5-minute empty room recording, usually recorded on the day of the experiment. The matrix of source weights for each block was used in a custom Matlab script to extract signals from V1, identified using the probabilistic maps of Wang et al. (2015). These signals were then imported into R for the main analysis, which was consistent with the EEG analysis described above. The outlier rejection procedure excluded 2.47% of trials for Experiment 3.

To make comparisons between groups of participants across time, we used a non-parametric cluster correction technique (Maris and Oostenveld, 2007) based on t-tests. Clusters were identified as temporally adjacent observations that were all statistically significant, and a summed t-value was calculated for each cluster. A null distribution was then generated by randomising group membership and recalculating the summed t-value for the largest cluster, and repeating this procedure 1000 times. Clusters were considered significant if they fell outside of the 95% confidence limits of the null distribution. We adapted this approach to test for significantly increasing suppression by conducting one-way t-tests between time points separated by 1000ms, and repeating the cluster correction procedure as described above.

4.4 Preregistration, data and code accessibility

Following a preliminary analysis of the data from Experiment 1, we preregistered our hypotheses and analysis plan for Experiments 2 and 3 on the Open Science Framework website. The preregistration document, along with raw and processed data, and analysis scripts, are publicly available at the project repository: https://osf.io/ab3yv/

5 Results

We began by reanalysing data from a steady-state visually evoked potential (SSVEP) experiment reported by Vilidaite et al. (2018). Participants viewed arrays of flickering gratings of varying contrasts. In some conditions a single grating orientation was present flickering at 7Hz, whereas in other conditions a high contrast 'mask' was added at right angles to the target gratings, and flickering at 5Hz. The left panel of Figure 1a shows contrast response functions with and without the mask - the presence of the mask reduces the 7Hz response to the target (blue squares are below the black circles; significant main effect of mask contrast, $F(1,99) = 26.52$, $p < 0.001$). Similarly, the right panel of Figure 1a shows that the 5Hz response to the mask was itself suppressed by the presence of high contrast targets (main effect of target contrast on the mask response, $F(2.92,288.63) = 46.77$, $p < 0.001$; note that the data from the masking conditions were not reported by Vilidaite et al. (2018)). At both frequencies, responses were localised to the occipital pole (see insets).

We then performed a timecourse analysis, in which we analysed each 11-second trial using a sliding 1-second time window. The top panel of Figure 1c shows the response at the target frequency (7Hz) to a single stimulus of 32% contrast (black), and the response at 7Hz when the 32% contrast mask is added (blue). For comparison, a baseline timecourse is also shown (grey), which was the response at 7Hz when a 5Hz stimulus

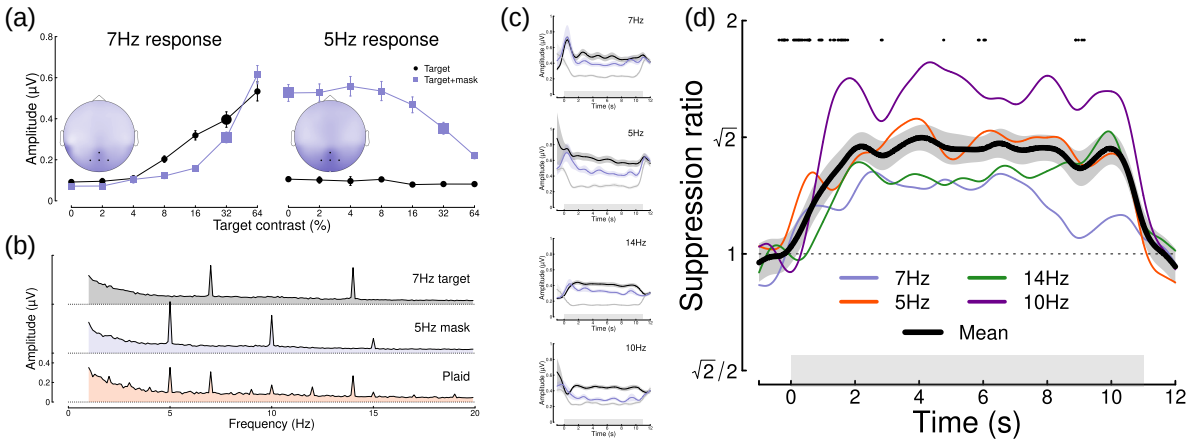

Figure 1: Summary of pilot analysis of data from Vilidiate et al. (2018). Panel (a) shows contrast response functions at the target frequency (7Hz, left) and the mask frequency (5Hz, right). Insets show the distribution of activity across the scalp, with points marking the electrodes over which signals were averaged (Oz, POz, O1 and O2). Panel (b) shows Fourier spectra for the single component stimuli and their combination (plaid). Note the strong second harmonic components at 14Hz and 10Hz. Panel (c) shows timecourses of frequency-locked responses to a single stimulus (black) and the plaid stimulus (blue), compared to baseline (grey). Panel (d) shows the timecourse of suppression at each frequency (7Hz, 5Hz, 14Hz, 10Hz) and their average (black curve). Points around y = 1.8 indicate a significantly increasing ratio. Error bars in panel (a) and shaded regions in panels (c,d) indicate ±1SE across N=100 participants, and grey rectangles indicate the timing of stimulus presentation. The larger symbols in panel (a) indicate the conditions used for subsequent analyses.

was shown (therefore controlling for attention, blinking etc.). Analogous responses are shown at three other frequencies - the mask frequency (5Hz), and the second harmonics of both target and mask frequencies (14Hz, 10Hz), at which strong responses were also found (see spectra in Figure 1b). The reduction in signal strength when the mask component is added illustrates the masking effect.

Taking the ratio of the two timecourses to calculate a masking index reveals that at 7Hz masking increases steeply during the first two seconds of stimulus presentation, and then plateaus for several seconds (blue trace in Figure 1d). A similar pattern is observed at 5Hz (red trace in Figure 1d), as well as at the second harmonics, with some variability in the timecourse across frequencies; for example, at 5Hz suppression peaks at around 4 seconds. The black trace shows the average masking ratio across all four frequencies, which rises steeply for just over two seconds and then stays approximately constant until stimulus offset. We conducted cluster-corrected t-tests between ratios separated by 1000ms, testing for an increase in suppression ratio across time (i.e. a one-sided test). Points at y = 1.8 in Figure 1d indicate time points where the ratio is significantly increasing, and occur mostly during the first 2 seconds of stimulus presentation.

Our initial reanalysis was promising, however the data were noisy despite the large sample size (of N=100), because each participant contributed only 8 trials (88 seconds) to each condition. We therefore preregistered two new experiments (see https://osf.io/4qudc) to investigate these effects in greater detail. These had a similar overall design to the Vilidaite et al. (2018) study, with some small changes intended to optimise the study (see Methods). The key differences were that we used shorter trials (because there were few changes in the latter part of the trials shown in Figure 1d), and also focussed all trials into a smaller number of conditions, such that each participant contributed 48 repetitions (288 seconds of data) to each of 4 conditions.

Figure 2 summarises the results of our EEG experiment testing a further 100 adult participants. Averaged EEG waveforms showed a strong oscillatory component at each of the two stimulus flicker frequencies (Figure 2a), which slightly lagged the driving signal. Signals were well-isolated in the Fourier domain (Figure 2b), and localised to occipital electrodes. Responses at 7Hz were weaker in the two masking conditions, showing significant changes in response amplitude for both the monocular ($t = 7.56$, $df = 87$, $p < 0.001$) and dichoptic

($t = 11.35$, $df = 87$, $p < 0.001$) masks. Dichoptic masking was significantly stronger than monocular masking ($t = 7.96$, $df = 87$, $p < 0.001$), and a similar pattern was evident at 5Hz.

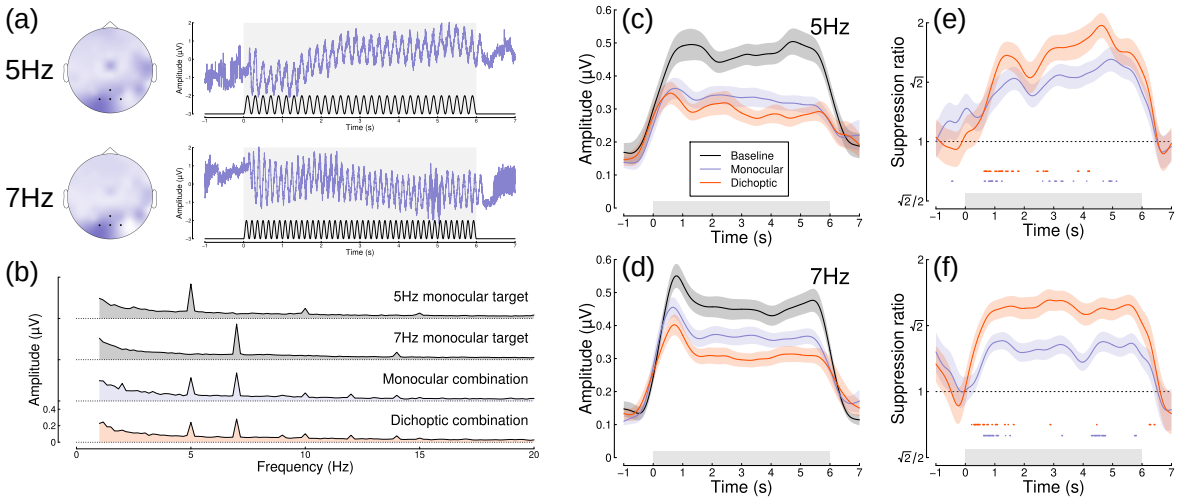

Figure 2: Summary of EEG results for N=100 adult participants. Panel (a) shows scalp topographies and averaged waveforms for 5Hz (top) and 7Hz (bottom) stimuli. The black sine wave trace in each panel illustrates the driving contrast modulation, and black points on the scalp topographies indicate electrodes Oz, O1, O2 and POz. Panel (b) shows the Fourier amplitude spectrum for each condition, with clear peaks at 5Hz and 7Hz. Panels (c,d) show timecourses at each frequency for the baseline condition (black), and the monocular (blue) and dichoptic (red) masking conditions. Panels (e,f) show suppression ratios as a function of time for each mask type, with points around y = 0.8 indicating a significantly increasing ratio. Shaded regions in panels (c-f) span ±1SE across participants, and light grey rectangles indicate the period of stimulus presentation.

The timecourse at both flicker frequencies showed an initial onset transient, and was then relatively stable for the 6 seconds of stimulus presentation (Figure 2c,d). The ratio of target only to target + mask conditions increased over time (Figure 2e,f) for both mask types. At 5Hz the increase in masking continued over the first 5 seconds of stimulus presentation (Figure 2e; points at y = 0.8 indicate significantly increasing suppression), whereas at 7Hz the increase occurred primarily during the first second after onset (Figure 2f). These differences across frequency are consistent with the pilot data (see Figure 1d). Both monocular and dichoptic masks produced similar timecourses of suppression. Overall, this second study confirmed that normalization increases during the first few seconds of a steady-state trial, and extends this finding to dichoptic mask arrangements.

Next we repeated the experiment on 20 participants using a 248-channel whole-head cryogenic MEG system. Half of the participants had a diagnosis of autism, and the remainder were age- and gender-matched controls. Source localisation using a linearly constrained minimum variance (LCMV) beamformer algorithm (Van Veen et al., 1997) showed strong localisation of steady-state signals at the occipital pole (see Figure 3a), and in the Fourier domain (Figure 3b). Responses from the most responsive V1 vertex showed a similar timecourse to those of the EEG experiments at both frequencies (Figure 3c,d), and showed increasing suppression during the first few seconds of stimulus presentation (Figure 3e,f). The normalization reweighting effect was again clearest at 5Hz, especially for the dichoptic condition (red curve in Figure 3e). This confirms that the reweighting effects can occur as early as primary visual cortex, consistent with findings from neurophysiology (Aschner et al., 2018). However the data are more variable than for our EEG experiments, and had fewer significant clusters, owing to the smaller sample size for this dataset.

To investigate whether normalization reweighting effects differ with respect to autistic traits, we then split each dataset (averaged across temporal frequency) using median AQ score (for the EEG experiments) or according to diagnostic group (autism vs controls) for the MEG data. Figure 4a-c shows distributions of AQ scores for each experiment, and indicates for the pilot and EEG data which participants were in the high

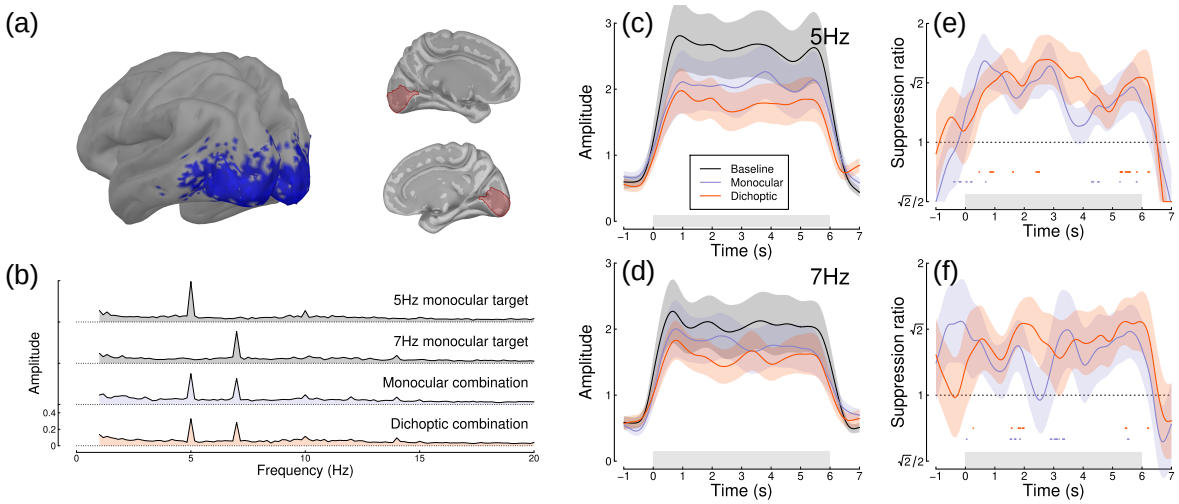

Figure 3: Summary of MEG results for N=20 adults. Panel (a) shows average SSVEP response in source space, thresholded at SNR=2 (blue, left), and locations of the V1 ROI on the medial surface of both hemispheres (right, red). Panel (b) shows the Fourier spectra for the four experimental conditions, from the most responsive vertex in V1. Panels (c,d) show timecourses at 5Hz and 7Hz, and panels (e,f) show suppression ratios for the monocular and dichoptic conditions at each frequency, with points around y = 0.8 indicating a significantly increasing ratio. Shaded regions in panels (c-f) indicate ±1SE across participants, and light grey rectangles indicate the period of stimulus presentation.

(purple) and low (green) AQ groups. The median AQ scores were 14 for the pilot data, and 18 for the EEG data. In the MEG experiment, AQ scores for the autism group (mean 36.1) and the control group (mean 16.7) were significantly different ($t = 6.00$, $df = 14.2$, $p < 0.001$), with minimal overlap (one participant with an autism diagnosis had an AQ score marginally lower than the highest AQ scores from the control group). These distributions are consistent with previous results for AQ (Baron-Cohen et al., 2001).

We compared the timecourse of suppression between groups using a nonparametric cluster correction approach (Maris and Oostenveld, 2007) to control the type I error rate. Significant clusters are indicated at y = 0.8 in panels d-h of Figure 4. Despite some occasionally significant clusters, there is no clear or consistent difference between groups across our three data sets. In particular, none of the significant clusters occur during the first few seconds of stimulus onset, when reweighting takes place. We also compared suppression ratios calculated on Fourier components for the full trial, and found no significant effects of autism on suppression strength. For Experiment 1 we assessed the first and second harmonics separately, but also found no AQ-related differences. We therefore conclude that autism/AQ score is not associated with normalization reweighting, or the strength of suppression more generally.

6 Discussion

We found evidence of dynamic normalization reweighting across three separate datasets. Suppression increased significantly during the first 2-5 seconds of stimulus presentation, though with some variation across temporal frequency. Reweighting had a similar timecourse for monocular and dichoptic stimulus presentation, and was apparent as early as V1. We did not find compelling differences associated with autism, or high vs low autistic traits. In the remainder of this section we will discuss possible explanations for temporal frequency differences, evidence for inhibitory differences in autism, and more general implications of dynamic normalization reweighting.

One important question is whether the dynamic increase in suppression can be explained by the stimulus onset transient. This is a possibility that cannot be ruled out for some of our data. For example, the steep increase in suppression in Figure 2f has a similar timecourse to the onset transient in Figure 2d. However, there are

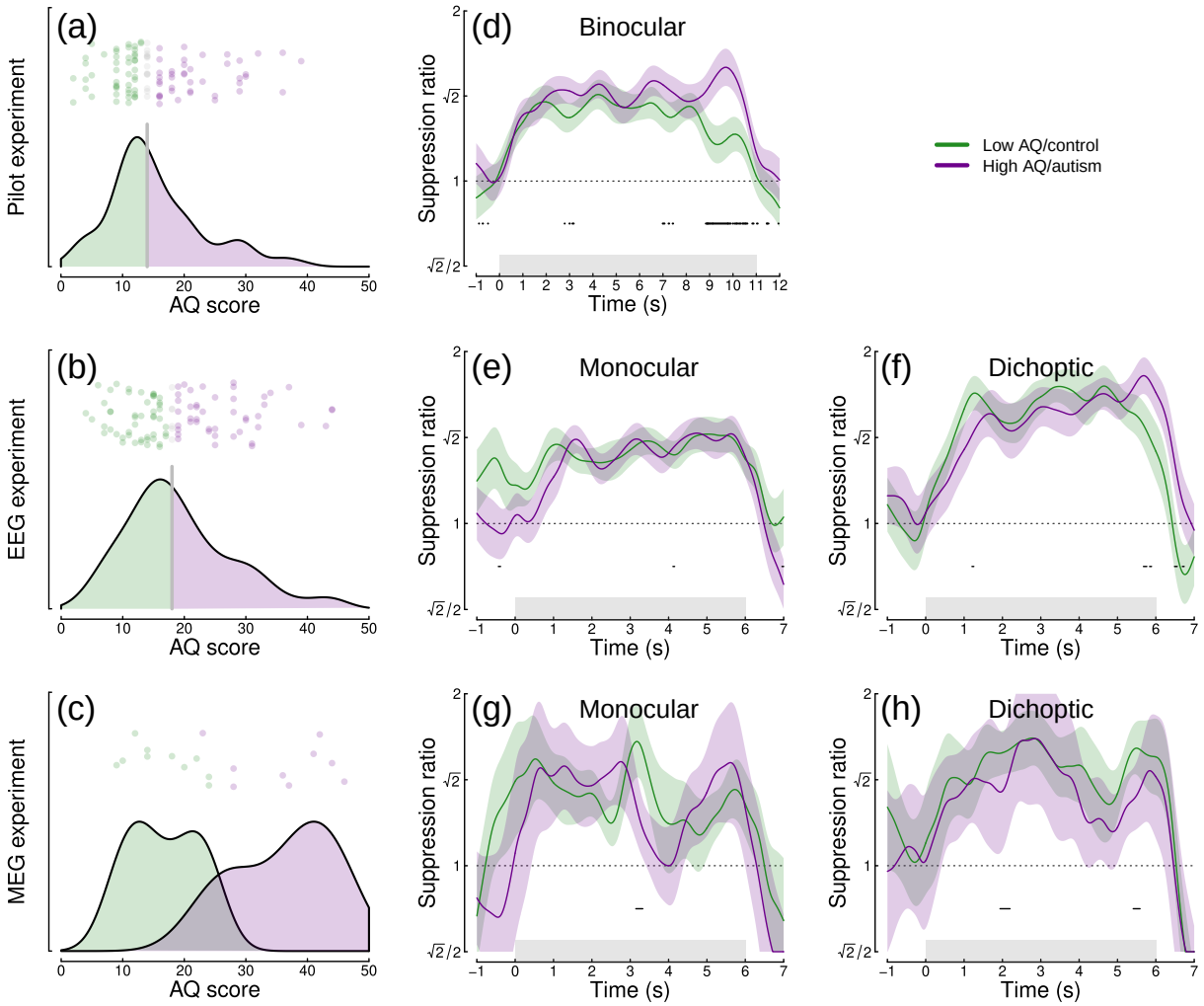

Figure 4: Analysis of the effect of autistic traits on normalization reweighting. Panels (a-c) show distributions of AQ scores across the three data sets. Panels (d-h) show timecourses of suppression averaged across stimulation frequency, and split by AQ score (d-f) or autism status (g, h). Panels (d,e,g) are for binocular or monocular presentation, and panels (f,h) are for dichoptic presentation. Shaded regions in panels (d-h) indicate ±1SE across participants, and black points at y = 0.8 indicate significant differences between groups.

also counterexamples where suppression continues to increase well beyond the first 1 second of stimulus presentation (e.g. Figure 2e). It is currently unclear why there appear to be such substantial differences between temporal frequency conditions, especially with such similar frequencies (5 and 7Hz). However the differences are relatively consistent across experiments. For example, 5Hz flicker produces a more gradual increase in suppression across all three data sets, compared with 7Hz flicker. These differences may be a consequence of visual channels with different temporal tuning interacting with the stimulation frequency, as well as any nonlinearities that govern suppression. Or there could be an asymmetry, whereby the relative temporal frequency between the two stimulus components affects the character of suppression (Liza and Ray, 2022). We hope to be able to model these effects in the future, for example by using dynamic models of early vision that incorporate time-lagged gain control (e.g. Zhou et al., 2019).

We did not observe clear differences in the timecourse between monocular and dichoptic suppression. This is important, because the dichoptic arrangement bypasses early stages of processing before the cortex (e.g. the retina and lateral geniculate nucleus). It suggests that the dynamic increases in suppression occur in the cortex, consistent with our MEG data that find evidence of reweighting in V1 (see Fig 3), and with previous neurophysiological work (Aschner et al., 2018). It is currently unclear whether these effects originate in V1, or might involve feedback from higher areas. The similarity between monocular and dichoptic effects also differs from work on adaptation to individual mask components. In both physiological (Li et al., 2005; Sengpiel and Vorobyov, 2005) and psychophysical (Baker et al., 2007) paradigms, adapting to a dichoptic mask reduces its potency, whereas adapting to a monocular mask has little or no effect. Normalization reweighting offers an explanation for why monocular masks presented in isolation do not adapt: if suppressive weights are determined by co-occurrence of stimuli, presentation of an isolated mask will have little effect. However this cannot explain the dichoptic adaptation effects without invoking additional binocular processes, such as competition between summing and differencing channels (e.g. May et al., 2012).

The relationship between normalization reweighting and other forms of visual plasticity is currently unclear. One phenomenon that might be closely related to our dichoptic effect is the change in interocular suppression that occurs when one eye is patched for a period of time (Lunghi et al., 2011). In the patching paradigm, the inputs to the two eyes are uncorrelated while one eye is patched, which the normalization reweighting model predicts should reduce suppression between the eyes. Most studies using patching have focussed on the resulting imbalance between the patched and non-patched eye, in which the patched eye contributes more to binocular single vision than the non-patched eye. In principle this could be due to increased suppression of the non-patched eye (inconsistent with normalization reweighting), or reduced suppression of the patched eye (consistent with normalization reweighting). It is difficult to distinguish these possibilities using paradigms that assess the balance between the two eyes, such as the binocular rivalry paradigm from the original Lunghi et al. (2011) study. However subsequent work has shown that patching increases the patched eye's response (Zhou et al., 2015), and reduces both dichoptic masking (Baldwin and Hess, 2018) and levels of the inhibitory neurotransmitter GABA (Lunghi et al., 2015). All of these findings are consistent with a reweighting account.

Autism is composed of a set of heterogenous symptoms and characteristics, and normalization reweighting may have a more specific relationship to some aspects of autism, rather than autism per se. For this reason, we also examined relationships with the sensory perception quotient (SPQ) to examine whether sensory experiences specifically were related to normalization reweighting. SPQ scores showed significant negative correlation with AQ for the data sets from Experiments 2 and 3 (EEG data, r = -0.35, $p < 0.001$; MEG data, r = -0.57, $p = 0.011$) with effect sizes comparable to those reported previously (Tavassoli et al., 2014). We also conducted an exploratory analysis of the EEG data from Experiment 2, splitting participants by SPQ instead of AQ. However this analysis did not reveal any convincing differences in normalization reweighting either. Our preregistration also proposed to replicate our earlier finding of a reduced second harmonic response in participants with autism/high AQ scores. However the changes to the experimental design greatly reduced the second harmonic response in both experiments, such that it could not be observed reliably (see Figures 2b and 3b). We were therefore not confident in conducting this analysis. We suspect that the increase in spatial frequency from 0.5 c/deg in the Vilidaite et al. (2018) study to 2 c/deg here is most likely responsible for the dramatically reduced second harmonic response.

The idea that the dynamic balance of inhibition and excitation might be different in autism (Rosenberg et al., 2015; Rubenstein and Merzenich, 2003) has compelling face validity. For example, individuals with

autism often report difficulties with changes in their sensory environment, which might be due to gain control processes failing to adapt appropriately. Indeed, there is experimental evidence of reduced adaptation across various domains (Pellicano et al., 2007; Turi et al., 2015), which is predicted by some autism models (Pellicano and Burr, 2012). However this appears not to extend to changes in normalization reweighting, despite the link between reweighting and adaptation (Westrick et al., 2016).

6.1 Conclusions

We investigated the timecourse of normalization reweighting across three datasets, with a total of 220 participants. We found clear evidence that suppression increases during the first 2-5 seconds of stimulus presentation, though there were differences across frequency that are currently unexplained. We did not find evidence of autism-related differences in either the magnitude or timecourse of suppression. Our results support an emerging theory that suppression is a dynamic process that allows sensory systems to recalibrate according to their recent history.

7 Acknowledgements

Supported by BBSRC grant BB/V007580/1 awarded to DHB and ARW. We are grateful to all of the participants who took part in the experiments reported here.

References

Aschner A, Solomon SG, Landy MS, Heeger DJ, Kohn A. 2018. Temporal contingencies determine whether adaptation strengthens or weakens normalization. *J Neurosci* **38**:10129–10142. doi:10.1523/JNEUROSCI.1131-18.2018

Baker DH. 2021. Statistical analysis of periodic data in neuroscience. *Neurons, Behavior, Data analysis, and Theory* **5**. doi:10.51628/001c.27680

Baker DH, Meese TS, Summers RJ. 2007. Psychophysical evidence for two routes to suppression before binocular summation of signals in human vision. *Neuroscience* **146**:435–448. doi:10.1016/j.neuroscience.2007.01.030

Baldwin AS, Hess RF. 2018. The mechanism of short-term monocular deprivation is not simple: Separate effects on parallel and cross-oriented dichoptic masking. *Sci Rep* **8**:6191. doi:10.1038/s41598-018-24584-9

Baron-Cohen S, Wheelwright S, Skinner R, Martin J, Clubley E. 2001. The autism-spectrum quotient (AQ): Evidence from asperger syndrome/high-functioning autism, males and females, scientists and mathematicians. *J Autism Dev Disord* **31**:5–17. doi:10.1023/a:1005653411471

Blakemore C, Campbell FW. 1969. On the existence of neurones in the human visual system selectively sensitive to the orientation and size of retinal images. *J Physiol* **203**:237–60. doi:10.1113/jphysiol.1969.sp008862

Cannon MW, Fullenkamp SC. 1991. Spatial interactions in apparent contrast: Inhibitory effects among grating patterns of different spatial frequencies, spatial positions and orientations. *Vision Res* **31**:1985–98. doi:10.1016/0042-6989(91)90193-9

Carandini M, Heeger DJ. 2011. Normalization as a canonical neural computation. *Nature Reviews Neuroscience* **13**:51–62. doi:10.1038/nrn3136

Dale AM, Fischl B, Sereno MI. 1999. Cortical surface-based analysis. I. Segmentation and surface reconstruction. *Neuroimage* **9**:179–94. doi:10.1006/nimg.1998.0395

Delorme A, Makeig S. 2004. EEGLAB: An open source toolbox for analysis of single-trial EEG dynamics including independent component analysis. *J Neurosci Methods* **134**:9–21. doi:10.1016/j.jneumeth.2003.10.009

Foley JM. 1994. Human luminance pattern-vision mechanisms: Masking experiments require a new model. *J Opt Soc Am A Opt Image Sci Vis* **11**:1710–9. doi:10.1364/josaa.11.001710

Foley JM, Chen CC. 1997. Analysis of the effect of pattern adaptation on pattern pedestal effects: A two-process model. *Vision Res* **37**:2779–88. doi:10.1016/s0042-6989(97)00081-3

Fonov V, Evans AC, Botteron K, Almli CR, McKinstry RC, Collins DL, Brain Development Cooperative Group. 2011. Unbiased average age-appropriate atlases for pediatric studies. *Neuroimage* **54**:313–27. doi:10.1016/j.neuroimage.2010.07.033

Freeman TCB, Durand S, Kiper DC, Carandini M. 2002. Suppression without inhibition in visual cortex. *Neuron* **35**:759–71. doi:10.1016/s0896-6273(02)00819-x

Gibson JJ, Radner M. 1937. Adaptation, after-effect and contrast in the perception of tilted lines. I. Quantitative studies. *Journal of Experimental Psychology* **20**:453–467. doi:10.1037/h0059826

Greenlee MW, Georgeson MA, Magnussen S, Harris JP. 1991. The time course of adaptation to spatial contrast. *Vision Res* **31**:223–36. doi:10.1016/0042-6989(91)90113-j

Haak KV, Fast E, Bao M, Lee M, Engel SA. 2014. Four days of visual contrast deprivation reveals limits of neuronal adaptation. *Curr Biol* **24**:2575–9. doi:10.1016/j.cub.2014.09.027

Heeger DJ. 1992. Normalization of cell responses in cat striate cortex. *Vis Neurosci* **9**:181–97. doi:10.1017/s0952523800009640

Hoekstra RA, Vinkhuyzen AAE, Wheelwright S, Bartels M, Boomsma DI, Baron-Cohen S, Posthuma D, Sluis S van der. 2011. The construction and validation of an abridged version of the autism-spectrum quotient (AQ-short). *J Autism Dev Disord* **41**:589–96. doi:10.1007/s10803-010-1073-0

Koh HC, Milne E, Dobkins K. 2010. Spatial contrast sensitivity in adolescents with autism spectrum disorders. *J Autism Dev Disord* **40**:978–87. doi:10.1007/s10803-010-0953-7

Kwon M, Legge GE, Fang F, Cheong AMY, He S. 2009. Adaptive changes in visual cortex following prolonged contrast reduction. *J Vis* **9**:20.1–16. doi:10.1167/9.2.20

Legge GE. 1979. Spatial frequency masking in human vision: Binocular interactions. *J Opt Soc Am* **69**:838–47. doi:10.1364/josa.69.000838

Li B, Peterson MR, Thompson JK, Duong T, Freeman RD. 2005. Cross-orientation suppression: Monoptic and dichoptic mechanisms are different. *J Neurophysiol* **94**:1645–50. doi:10.1152/jn.00203.2005

Liza K, Ray S. 2022. Local interactions between steady-state visually evoked potentials at nearby flickering frequencies. *J Neurosci* **42**:3965–3974. doi:10.1523/JNEUROSCI.0180-22.2022

Lunghi C, Burr DC, Morrone C. 2011. Brief periods of monocular deprivation disrupt ocular balance in human adult visual cortex. *Curr Biol* **21**:R538–9. doi:10.1016/j.cub.2011.06.004

Lunghi C, Emir UE, Morrone MC, Bridge H. 2015. Short-term monocular deprivation alters GABA in the adult human visual cortex. *Curr Biol* **25**:1496–501. doi:10.1016/j.cub.2015.04.021

MacLennan K, O'Brien S, Tavassoli T. 2022. In our own words: The complex sensory experiences of autistic adults. *J Autism Dev Disord* **52**:3061–3075. doi:10.1007/s10803-021-05186-3

Maris E, Oostenveld R. 2007. Nonparametric statistical testing of EEG- and MEG-data. *J Neurosci Methods* **164**:177–90. doi:10.1016/j.jneumeth.2007.03.024

Mather G, Pavan A, Campana G, Casco C. 2008. The motion aftereffect reloaded. *Trends Cogn Sci* **12**:481–7. doi:10.1016/j.tics.2008.09.002

May KA, Zhaoping L, Hibbard PB. 2012. Perceived direction of motion determined by adaptation to static binocular images. *Curr Biol* **22**:28–32. doi:10.1016/j.cub.2011.11.025

Meese TS, Baker DH. 2009. Cross-orientation masking is speed invariant between ocular pathways but speed dependent within them. *Journal of Vision* **9**:2. doi:10.1167/9.5.2

Pellicano E, Burr D. 2012. When the world becomes 'too real': A bayesian explanation of autistic perception. *Trends Cogn Sci* **16**:504–10. doi:10.1016/j.tics.2012.08.009

Pellicano E, Jeffery L, Burr D, Rhodes G. 2007. Abnormal adaptive face-coding mechanisms in children with autism spectrum disorder. *Curr Biol* **17**:1508–12. doi:10.1016/j.cub.2007.07.065

Petrov Y. 2005. Two distinct mechanisms of suppression in human vision. *Journal of Neuroscience* **25**:8704–8707. doi:10.1523/jneurosci.2871-05.2005

Rosenberg A, Patterson JS, Angelaki DE. 2015. A computational perspective on autism. *Proc Natl Acad Sci U S A* **112**:9158–65. doi:10.1073/pnas.1510583112

Rosenhall U, Nordin V, Sandström M, Ahlsén G, Gillberg C. 1999. Autism and hearing loss. *J Autism Dev Disord* **29**:349–57. doi:10.1023/a:1023022709710

Rubenstein JLR, Merzenich MM. 2003. Model of autism: Increased ratio of excitation/inhibition in key neural systems. *Genes Brain Behav* **2**:255–67. doi:10.1034/j.1601-183x.2003.00037.x

Sandhu TR, Reese G, Lawson RP. 2020. Preserved low-level visual gain control in autistic adults. *Wellcome Open Research* **4**. doi:10.12688/wellcomeopenres.15615.1

Schallmo M-P, Kolodny T, Kale AM, Millin R, Flevaris AV, Edden RAE, Gerdts J, Bernier RA, Murray SO. 2020. Weaker neural suppression in autism. *Nat Commun* **11**:2675. doi:10.1038/s41467-020-16495-z

Sengpiel F, Blakemore C. 1994. Interocular control of neuronal responsiveness in cat visual cortex. *Nature* **368**:847–50. doi:10.1038/368847a0

Sengpiel F, Vorobyov V. 2005. Intracortical origins of interocular suppression in the visual cortex. *J Neurosci*

25:6394–400. doi:10.1523/JNEUROSCI.0862-05.2005

Simmons DR, Robertson AE, McKay LS, Toal E, McAleer P, Pollick FE. 2009. Vision in autism spectrum disorders. *Vision Research* **49**:2705–2739. doi:10.1016/j.visres.2009.08.005

Tadel F, Baillet S, Mosher JC, Pantazis D, Leahy RM. 2011. Brainstorm: A user-friendly application for MEG/EEG analysis. *Comput Intell Neurosci* **2011**:879716. doi:10.1155/2011/879716

Tavassoli T, Hoekstra RA, Baron-Cohen S. 2014. The sensory perception quotient (SPQ): Development and validation of a new sensory questionnaire for adults with and without autism. *Mol Autism* **5**:29. doi:10.1186/2040-2392-5-29

Tavassoli T, Latham K, Bach M, Dakin SC, Baron-Cohen S. 2011. Psychophysical measures of visual acuity in autism spectrum conditions. *Vision Research* **51**:1778–1780. doi:10.1016/j.visres.2011.06.004

Turi M, Burr DC, Igliozzi R, Aagten-Murphy D, Muratori F, Pellicano E. 2015. Children with autism spectrum disorder show reduced adaptation to number. *Proc Natl Acad Sci U S A* **112**:7868–72. doi:10.1073/pnas.1504099112

Van de Cruys S, Vanmarcke S, Steyaert J, Wagemans J. 2018. Intact perceptual bias in autism contradicts the decreased normalization model. *Scientific Reports* **8**. doi:10.1038/s41598-018-31042-z

Van Veen BD, Drongelen W van, Yuchtman M, Suzuki A. 1997. Localization of brain electrical activity via linearly constrained minimum variance spatial filtering. *IEEE Trans Biomed Eng* **44**:867–80. doi:10.1109/10.623056

Vilidaite G, Norcia AM, West RJH, Elliott CJH, Pei F, Wade AR, Baker DH. 2018. Autism sensory dysfunction in an evolutionarily conserved system. *Proc Biol Sci* **285**:20182255. doi:10.1098/rspb.2018.2255

Wang L, Mruczek REB, Arcaro MJ, Kastner S. 2015. Probabilistic maps of visual topography in human cortex. *Cereb Cortex* **25**:3911–31. doi:10.1093/cercor/bhu277

Webster MA. 2015. Visual adaptation. *Annu Rev Vis Sci* **1**:547–567. doi:10.1146/annurev-vision-082114-035509

Westrick ZM, Heeger DJ, Landy MS. 2016. Pattern adaptation and normalization reweighting. *Journal of Neuroscience* **36**:9805–9816. doi:10.1523/jneurosci.1067-16.2016

Yiltiz H, Heeger DJ, Landy MS. 2020. Contingent adaptation in masking and surround suppression. *Vision Res* **166**:72–80. doi:10.1016/j.visres.2019.11.004

Zhou J, Baker DH, Simard M, Saint-Amour D, Hess RF. 2015. Short-term monocular patching boosts the patched eye's response in visual cortex. *Restor Neurol Neurosci* **33**:381–7. doi:10.3233/RNN-140472

Zhou J, Benson NC, Kay K, Winawer J. 2019. Predicting neuronal dynamics with a delayed gain control model. *PLoS Comput Biol* **15**:e1007484. doi:10.1371/journal.pcbi.1007484